METIS, THE MULTI ELEMENT TELESCOPE FOR IMAGING AND SPECTROSCOPY: AN INSTRUMENT PROPOSED FOR THE SOLAR ORBITER MISSION

E. Antonucci[(1)], V. Andretta[(2)], S. Cesare[(3)], A. Ciaravella[(4)], G. Doschek[(5)], S. Fineschi[(6)], S. Giordano[(7)], P. Lamy[(8)], D. Moses[(9)], G. Naletto*[(10,11)], J. Newmark[(12)], L. Poletto[(13)], M. Romoli[(14)], S. Solanki[(15)], D. Spadaro[(16)], L. Teriaca[(17)], L. Zangrilli[(18)]

[(1)]Istituto Nazionale di Astrofisica (INAF) - Osservatorio Astronomico di Torino, Via Osservatorio,20, I-10025 Pino Torinese TO, Italy. E-mail: antonucci@to.astro.it
[(2)]INAF - Osservatorio Astronomico di Capodimonte, Salita Moiariello, 16, I-80131Napoli NA, Italy. E-mail: andretta@oacn.inaf.it
[(3)]Thales Alenia Space, Strada Antica di Collegno, 253, I-10146 Torino TO, Italy. E-mail: stefano.cesare@thalesaleniaspace.com
[(4)]INAF - Osservatorio Astronomico di Palermo, Piazza del Parlamento 1, I-90134 Palermo PA, Italy. E-mail: ciarave@astropa.unipa.it
[(5)]U.S. Naval Research Laboratory, 4555 Overlook Ave., SW, Washington, DC 20375, USA. E-mail: george.doschek@nrl.navy.mil
[(6)]Same affiliation of (1. E-mail: fineschi@to.astro.it
[(7)]Same affiliation of (1). E-mail: giordano@to.astro.it
[(8)]Laboratoire d'Astrophysique de Marseille, Pôle de l'Etoile Site de Château-Gombert 38, rue Frédéric Joliot-Curie, F-13388 Marseille cedex 13, France. E-mail: philippe.lamy@oamp.fr
[(9)]Same affiliation of (5). E-mail: moses@nrl.navy.mil
[(10)]Department of Information Engineering, University of Padova, Via Gradenigo, 6/B, I-35131 Padova PD, Italy. E-mail: naletto@dei.unipd.it
[(11)]CNR-INFM-LUXOR, Via Gradenigo, 6/B, I-35131 Padova PD, Italy.
[(12)]Same affiliation of (5). E-mail: newmark@nrl.navy.mil
[(13)]Same affiliation of (11). E-mail: poletto@dei.unipd.it
[(14)]Dipartimento di Astronomia e Scienza dello Spazio - Università degli Studi di Firenze, Largo Enrico Fermi 2, I-50125 Firenze FI, Italy. E-mail: romoli@arcetri.astro.it
[(15)]Max-Planck-Institut fur Sonnensystemforschung, Max-Planck-Str. 2, D-37191 Katlenburg-Lindau, Germany. E-mail: solanki@linmpi.mpg.de
[(16)]INAF - Osservatorio Astrofisico di Catania, Via S. Sofia 78, I-95123 Catania, Italy. E-mail: dspadaro@oact.inaf.it
[(17)]Same affiliation of (15). E-mail: teriaca@mps.mpg.de
[(18)]Same affiliation of (1). E-mail: zangrilli@to.astro.it

** Corresponding author: e-mail: naletto@dei.unipd.it*

ABSTRACT

METIS, the Multi Element Telescope for Imaging and Spectroscopy, is an instrument proposed to the European Space Agency to be part of the payload of the Solar Orbiter mission. The instrument design has been conceived for performing extreme ultraviolet (EUV) spectroscopy both on the solar disk and off-limb, and near-Sun coronagraphy and spectroscopy.
The proposed instrument suite consists of three different interconnected elements, COR, EUS and SOCS, sharing the same optical bench, electronics, and S/C heat shield aperture. COR is a visible-EUV multiband coronagraph based on a classical externally occulted design. EUS is the component of the METIS EUV disk spectrometer which includes the telescope and all the related mechanisms. Finally, SOCS is the METIS spectroscopic component including the dispersive system and the detectors. The capability of inserting a small telescope collecting coronal light has been added to perform also EUV coronal spectroscopy.
METIS can simultaneously image the visible and ultraviolet emission of the solar corona and diagnose, with unprecedented temporal coverage and space resolution the structure and dynamics of the full corona in the range from 1.2 to 3.0 (1.6 to 4.1) solar radii ($R_\odot$, measured from Sun centre) at minimum (maximum) perihelion during the nominal mission. It can also perform spectroscopic observations of the solar disk and out to 1.4 $R_\odot$ within the 50-150 nm spectral region, and of the geo-effective coronal region 1.7-2.7 $R_\odot$ within the 30-125 nm spectral band.

1. INTRODUCTION

Solar Orbiter is a mission of the European Space Agency (ESA) planned to be launched on 2015 to provide the next major step forward in the exploration of the Sun and the heliosphere after the successful ESA missions Ulysses and SOHO, as well as the NASA TRACE, RHESSI, STEREO and the Japanese Hinode. In 2007 Solar Orbiter has been included, along with the NASA Sentinels mission, in the ESA-NASA Helio-physical Explorers **(**HELEX**)** program which exploits the synergy of the two missions to answer fundamental questions about the Sun-heliosphere linkage.
ESA has very recently issued an Announcement of Opportunity (AO) for submitting scientific investigations for the Solar Orbiter mission: in response to this AO, we have proposed the *Multi Element Telescope for Imaging and Spectroscopy* (METIS) investigation. This instrument suite has been conceived with the purpose of performing both extreme ultraviolet (EUV) spectroscopy on the solar disk and off-limb, and near-Sun coronagraphy and spectroscopy. The main scientific motivation of METIS is the attempt of addressing the three key scientific questions identified as the focus of the HELEX program: the origin and heating/acceleration of the solar wind streams; the origin, acceleration and transport of the solar energetic particles; and the transient ejection of coronal mass and its evolution in the inner heliosphere. The selection of the Solar Orbiter payload is expected within the end of the year.

The METIS suite consists of three different elements, sharing the same optical bench, electronics, power supply and S/C heat shield aperture. The three elements are identified as:

a. COR: a visible and EUV coronagraph
b. EUS: an EUV disk spectrometer
c. SOCS: the Solar Orbiter Coronal Spectrometer

In an approach oriented to the best sharing of tasks between the imaging and the spectroscopic investigation of the Sun, and in particular of the solar corona, and to the best coordination between them, METIS is a highly integrated instrument. The proposed approach seems to be the most effective to obtain the highest scientific return, while minimizing the overall resource allocation. In fact, the proposed architecture takes advantage of the commonality between the different elements that constitute the suite.
In the next sections a brief description of the METIS suite and of each element is given.

2. THE METIS SUITE

A pictorial view of METIS is shown in Fig. 1. Here the common optical bench on which all the optical elements are mounted is shown. Also the instrument aperture and

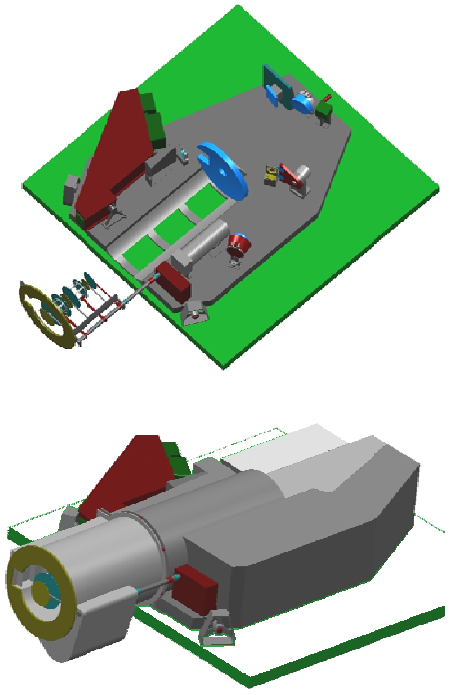

Fig. 1. METIS suite layout. Top: view of the optical elements and bench (in gray) laying on the spacecraft panel (in green); the brown box is the SOCS element. Bottom: view of the instrument with baffles and enclosure.

the coronagraph external occulting system protruding from the optical bench and entering in the spacecraft (S/C) heat shield (not shown in figure), are evident. The total external envelope of METIS is 1403×830×264 mm^3. The instrument power supply and data handling electronics is contained in a not shown 220×250×350 mm^3 box separated from the optical bench to be suitably located on the S/C.

2.1. COR: a visible and EUV coronagraph

COR is an externally occulted coronagraph designed for performing broad-band polarization imaging of the visible K-corona, narrow-band imaging of the UV corona in the HI Lyman-α (121.6 nm) line, and narrow-band imaging of the EUV corona in the HeII Lyman-α (30.4 nm) line. COR is planned to observe in an annular field of view (FOV) between 1.2 $R_\odot$ and 3.0 $R_\odot$ at 0.226 AU perihelion (perihelion will change during the mission).
The coronagraph critical issue of solar disk light rejection is taken care of by means of a novel optical design for a reflecting coronagraph, widely used in traditional externally occulted coronagraphs. This optical design has been thoroughly studied in the design of the SCORE coronagraph developed for the sub-orbital mission HERSCHEL [1-4]. A combination of

multilayer coating of the mirrors, optimized to enhance reflectivity in the EUV He line, and of band-pass filters contribute to the capability of imaging the solar corona in three different wavelength bands by means of a single telescope. These mirrors are coated with multilayer optimized for 30.4 nm, but that maintains good reflectivity at 121.6 nm and in the visible.

A schematic of the COR element is shown in Fig. 2, and its optical specifications are summarized in Tab. 1. COR is based on a classical externally occulted design, in which light enters through the external occulter (EO) aperture, that provides the Sun disk occultation, located at the outside panel of the S/C heat shield. The EO is a fixed triple disk system that ensures both thermal protection for the optics and optimal stray-light rejection; it is supported by a suitable truss fixed to the optical bench, protruding from the S/C instrument bay inside the heat shield.

An annular shaped Sun-disk rejection mirror (M0) back reflects the sun disk light through the front aperture to minimize the thermal load inside the instrument, and leaves the coronal light reaching the telescope through a hole at its center located in the shadow of the external occulter. This hole has also the optical function of COR aperture stop.

Coronal light passing through M0 reaches the COR telescope, which consists of aspherical primary (M1) and secondary (M2) mirrors in off-axis Gregorian mount. The image of EO produced by M1 is blocked by a stop called internal occulter (IO): its function is to block the disk solar light diffracted by EO which could be a strong source of noise for the system. In addition, M1 forms an image of the aperture stop on the plane of M2: this image, potential source of stray light inside the instrument, is collected by a light trap behind M2, acting as the so-called Lyot stop. The expected stray light level on the detector is given in Tab. 1.

The coronal radiation reflected by M2 impinges the filter wheel. The filter wheel mechanism (FM) accommodates two filters: a narrow band multilayer filter (HF) optimized to transmit the HI 121.6 nm line and to reflect the visible light (VL), and an aluminum low pass filter (HeF) to select the HeII 30.4 nm line. With HF inserted, the UV HI 121.6 nm corona and the VL K-corona are imaged simultaneously, respectively on the UV detector (UVD) and on the VL detector (VLD). With HeF inserted, only the EUV HeII 30.4 nm is imaged on the UVD. In the VL channel, before reaching the detector after the filter reflection, the radiation is also processed by an achromatic polarimeter (PL) for measuring the linear polarized brightness.

COR has the capability of being operative also during spacecraft off-pointing by means of a mechanism that inserts an additional external occulter system, called extended external occulter (EEO). The latter is a five disks system large enough to prevent sun disk light from entering the coronagraph aperture stop also when the

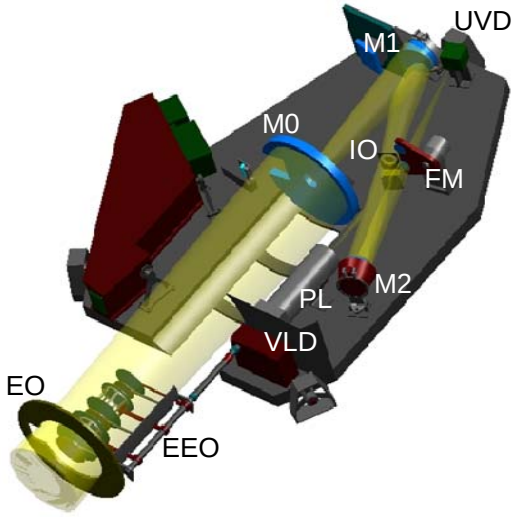

Fig. 2. Schematic of the COR optical path inside METIS.

Tab. 1. COR optical specifications.

Field of View	Annular Sun-centered 1.2-3.0 $R_\odot$ @ 0.226 AU 1.6-4 $R_\odot$ @ 0.3 AU
Telescope type	Externally occulted off-axis Gregorian
Effective focal length	400 mm
External occulter (EO)	Triple disk type Annular sector: inner Ø: 80.3 mm, outer Ø: 180 mm
Sun-light Rejection mirror (M0)	Toric annular sector; Ø: 264 mm Substrate: SiC Coating: SiC
Stop aperture	Ø: 40 mm
Primary mirror (M1)	Off axis ellipsoidal; Ø: 80 mm Substrate: quartz Coating: multilayer
Secondary mirror (M2)	Off axis ellipsoidal; Ø:57.4 mm Substrate: quartz Coating: multilayer
Filter mechanism (FM)	HF: Al+MgF_2 HeF: Al
Spatial resolution	see Fig. 3
Stray light levels	VL: < 10^{-9} UV, EUV: < 10^{-7}
Wavelength band-pass	VL: 450-650 nm UV HI (121.6 ± 10) nm EUV HeII (30.4 ± 2) nm
UV Detector	IAPS Scale factor: 12.9 arcsec/pixel Format: 2048×2048 Pixel size: square, 25 µm side
VL Detector	APS Scale factor: 12.9 arcsec/pixel Format: 2048×2048 Pixel size: square, 25 µm side

S/C is off-pointed by 1.25°. In case of off-pointing, COR FOV will not be symmetrical with respect to Sun center.
The VLD considered for COR is a custom developed Active Pixel Sensor (APS). The choice of an APS over a CCD is driven by the harsh radiation environment of Solar Orbiter. Until recently, the readout noise of APS detectors was well above the VLD requirements needed for this application; however, now a readout noise of 10 e^- is in the current technological capability of European companies. Due to the relatively long acquisition frame period, the APS has to be operated at low temperatures (of the order of –40°C) and therefore must be equipped with a thermo-electric cooler device and a suitable radiator.
The COR-UV detector works in photon counting mode and will be an intensified APS (IAPS). A description of the intensified detectors used on METIS is given in Sect. 3.

The optical performance of COR is given in terms of spatial resolution on the focal plane for all three channels in Fig. 3 The effect of diffraction due to the vignetting of the entrance pupil by the external occulter is also evaluated and taken into account.
To estimate COR efficiency, the effective areas in the three COR channels have been calculated, taking into account the vignetting function, the mirror coatings, the filter transmission and detector efficiencies. The COR count rate (see Fig. 4) has then been estimated by means of the coronal radiances values of the K-corona polarized brightness and HI Ly-α obtained at solar minimum with SOHO LASCO and UVCS [5,6], whilst the HeII Ly-α count rates are derived from modeled radiances. For K-corona PB images, the statistics required for achieving 1% accuracy is at least 10^4 counts; for UV/EUV images the accuracy required is 10%, corresponding to at least 10^2 counts.

2.2. EUS: an EUV disk spectrometer

EUS is the component of the METIS EUV disk spectrometer which includes the telescope and all the related mechanisms. Since EUS instantaneous FOV is rather small, a rotation of the EUS telescope around an axis passing through its vertex is foreseen to scan the sun disk along the East-West direction in order to cover a large part of the sun disk. By means of another mechanism, a mirror can be inserted on the EUS optical path to image selected portions of the solar corona, instead of the disk, on the spectrometer entrance slit. This allows to perform spectroscopic measurement also on the corona, and not only on the Sun disk. In both cases, after the entrance slit, light enters the SOCS element, which includes the dispersive element and the detectors of the METIS spectrometer. The adopted two-element design allows to maintain a high system

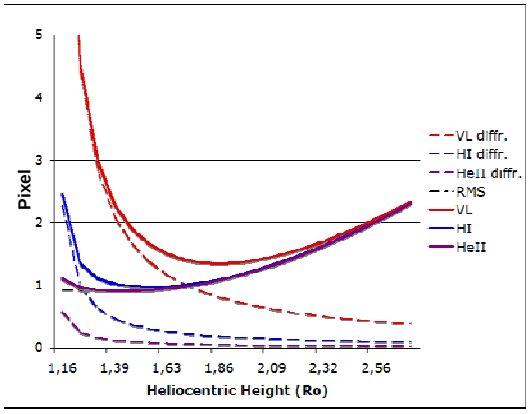

Fig. 3. COR spatial resolution as a function of helio-centric height for all three wavelength bands. The curves include the optical aberrations and an estimate of the diffraction.

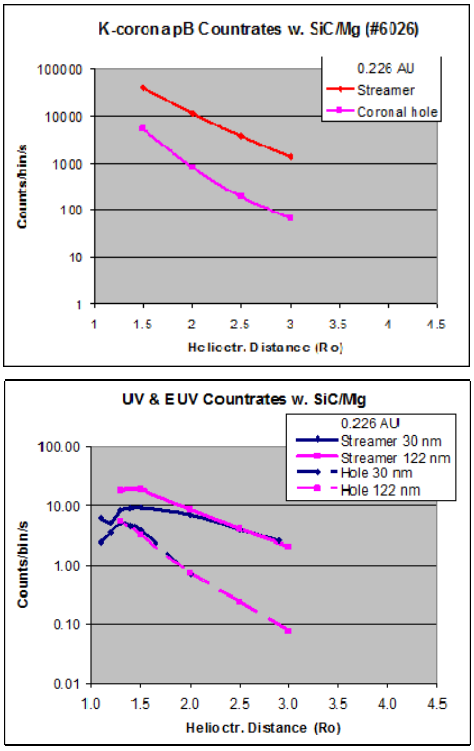

Fig. 4. Count-rates for observations from 0.22 AU. Top: polarized visible-light K-corona. Bottom: count rates for observations of the HI 122 nm and HeII 30 nm coronal emission.

efficiency since the number of reflections is reduced to the minimum.
A schematic of the EUS element is shown in Fig. 5, and its optical specifications are summarized in Tab. 2. Light from the sun disk passes through the METIS aperture on the S/C sun shield, through a cut-out on M0, and reaches the EUS telescope (ET), an off-axis parabola. Just behind ET, a heat trap (HT) is located. In

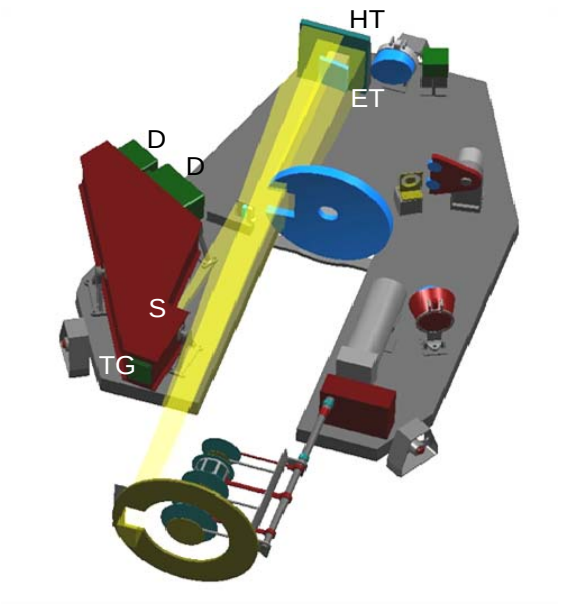

Fig. 5. Schematic of the EUS optical path inside METIS.

Tab. 2. EUS optical specifications.

Entrance aperture	50 mm × 60 mm
Telescope	Off-axis parabola 62 mm (⊥ to the slit) × 75 mm
Raster angle	±30 arcmin
Slit angular size	1.1 arcsec × 40 arcmin
Grating	TVLS 29 mm (⊥ to the grooves) × 40 mm
Central groove density	3600 mm^{-1}
Detectors	IAPS (both analog and photon counting)
Format	2048 × 2048
Pixel size	12 μm × 12 μm
Channel 1	
Spectral interval	96.8-109.0 nm (1st order) 48.4-54.5 nm (2nd order)
Spectral plate factor	5.96 pm /pixel (1st order) 2.98 pm /pixel (2nd order)
Spatial scale	1.2 arcsec/pixel
Channel 2	
Spectral interval	116.2-126.6 nm (1st order) 58.1-63.3 nm (2nd order)
Spectral plate factor	5.08 pm /pixel (1st order) 2.54 pm /pixel (2nd order)
Spatial scale	1.1 arcsec/pixel
Channel 3	
Spectral interval	151.6-158.4 nm (1st order) 75.8-79.2 nm (2nd order) 50.5-52.8 nm (3rd order)
Spectral plate factor	3.32 pm /pixel (1st order) 1.66 pm /pixel (2nd order) 1.11 pm /pixel (3rd order)
Spatial scale	1.0 arcsec/pixel

fact, to reduce the heat load entering the instrument, the mirror is made of high transparent quartz coated with a thin layer of either B_4C or SiC [7]: in this way, the mirror mainly reflects the EUV light of interest, but at the same time transmits the majority of visible and IR light arriving from the sun disk. The latter is the radiation bringing the higher thermal load, which is in this way collected by HT and then suitably dissipated. On the plane where ET forms the image of the solar disk, different entrance slits (S) can be placed by a suitable mechanism. From here, the radiation reaches a toroidal grating (TG) with variable-line-spaced grooves (TVLS grating) which gives a stigmatic spectrum of each of the points along the slit height on the focal plane. The TVLS grating design has been found to provide excellent off-axis imaging in configurations with magnification higher than unity, permitting high-quality performance in compact instrument packages [8,9]. Three bi-dimensional micro-channel plate (MCP) photon counting detectors (D) (see Sect. 3) are aligned on the spectral curve to acquire simultaneously the imaging spectra on six spectral intervals in the 1st and 2nd diffracted orders. We also expect observing third order lines on detector 3.

Aberrations are very low over all the spectrum, allowing to obtain a spatial resolution limited by the detector within 30 (instantaneous) × 17 (rastered) $arcmin^2$ FOV. Outside this FOV aberrations slightly increase, remaining anyway smaller than 3 pixels at the extremes.

EUS efficiency has been estimated taking into account the reflectivity of a B_4C coating, the grating diffraction efficiency and the detector efficiency. The reflectivity of ET is assumed to be 15% less than standard B_4C [10,11] reflectivity to account for the loss due to the required "thermal" transmitting capability of this mirror. Moreover, a conservative 50% peak diffraction efficiency of the grating has been considered for safety.

The photocathode selected for the photon counting IAPS detectors is KBr [12,13]. However, the visibility of 2nd and 3rd order spectral lines is definitely compromised unless the strongest 1st order contribution is reduced at the detector stage. Since the efficiency of the bare MCP is relatively high at short wavelengths, in order to enhance the contrast between 2nd and 1st order lines it has been decided to use a detector with a partially KBr coated and partially bare MCP: second order lines will be observed on the bare MCP portions, while first order lines will be observed on the KBr coated portions to reduce blending between orders. Moreover, since the radiance on the HI Ly-α line at 121.6 nm is 2-4 orders of magnitudes higher than that of the other lines on the same spectral channel, the portion of the MCP on which the HI Ly-α line falls will be uncoated, thus reducing the contrast by a factor ≈20. In addition, the HI Ly-α flux will be further reduced by a suitably located 10% transmission mesh, as successfully adopted in SUMER [11]. To summarize the global

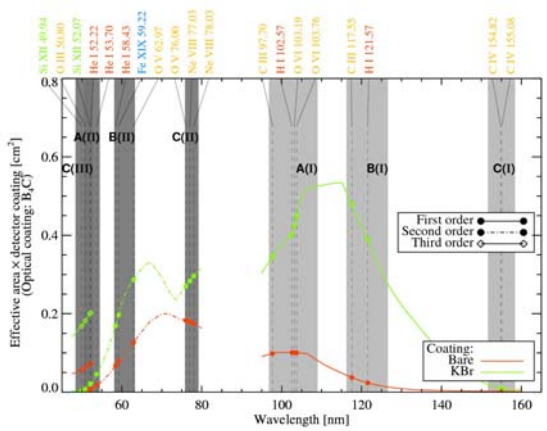

Fig. 6. EUS effective areas for the different MCP coating options. The gray areas correspond to the portions of the spectrum covered by the detectors.

efficiency performance of EUS, its estimated effective area is schematically shown in Fig. 6.

2.3. SOCS: the Solar Orbiter Coronal Spectrometer

SOCS is essentially an independent box which includes the dispersive system and the detectors of the METIS spectrometer. It consists of a fixed array of slits, a TVLS grating and a set of three independent detectors mounted on suitable positions to collect three different interesting portions of the solar spectrum. SOCS allows to perform the spectral analysis of both the Sun disk and corona. A multi-slit system has been implemented in order to allow simultaneous spectroscopic observations of different portions of the corona,. Essentially, in this case, there are four different slits at the SOCS entrance slit plane, which allow to analyze four different portions of the solar corona at different solar heights. Each slit produces its own spectrum, which is then collected by the SOCS detectors.

A schematic of the SOCS element is shown in Fig. 7, and its optical specifications are summarized in Tab. 3.

Light from the solar corona passing through the METIS aperture is collected by the insertable SOCS telescope (ST), a low resolution off-axis parabola, and an image is created at the entrance plane of the spectrometer where the field stop with four slits (S) is located. Coronal light passing through the slits is then diffracted by the TVLS grating (TG); the latter creates stigmatic spectral images of the different slits on the same detectors used by EUS.

The angular separation among the slits is such to bring the spectral lines of interest on the coated areas of the detector MCPs, to have the highest detection efficiency. The positions of the spectral lines on the three detectors are shown in Fig. 8.

Since the areas illuminated on TG for on-disk and coronal observations are different, a coating different from B_4C, which is optimal for disk spectroscopy but

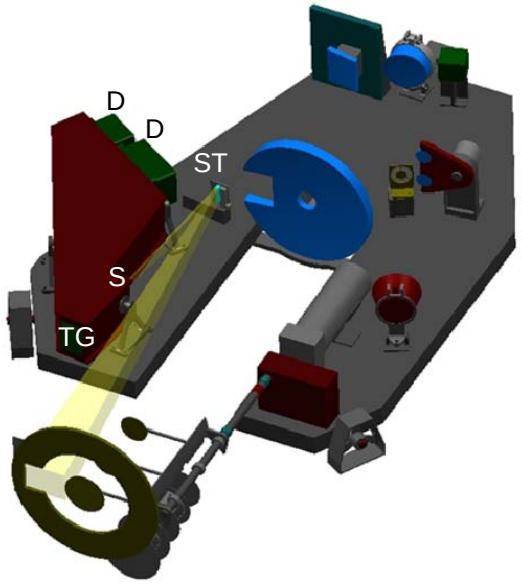

Fig. 7. Schematic of the SOCS optical path inside METIS.

Tab. 3. SOCS optical specifications.

Telescope	Off-axis parabola 20 mm (⊥ to the slit) × 40 mm
Slit angular size	22 arcsec × 2.5°
Number of slits	4
Slit radial distance from Sun center @ 0.22 AU	1.68 $R_\odot$ - 1.93 $R_\odot$ - 2.27 $R_\odot$ - 2.60 $R_\odot$
Detectors	IAPS
Format	2048 × 2048
Pixel size	12 μm × 12 μm
Channel 1	
Most intense lines	103.2-103.7 nm (OVI doublet)
Spectral plate factor	5.96 pm/pixel (1st order)
Spatial scale	4.4 arcsec/pixel
Channel 2	
Most intense line	121.6 nm (HI Ly-α)
Spectral plate factor	5.08 pm/pixel (1st order)
Spatial scale	4.1 arcsec/pixel
Channel 3	
Most intense line	30.4 nm (HeII, 5th order)
Spectral plate factor	0.66 pm/pixel (5th order)
Spatial scale	3.5 arcsec/pixel

not for the observations in the corona, can be adopted. Hence, for both ST and the portion of TG invested by coronal light, a multilayer coating optimized for the 30.4 nm HeII line and with high reflectivity also at 103.2-103.7 nm and at 121.6 nm [14,15,16] has been selected. As an example, the reflectivity of an optimized Mo-Si multilayer coating is shown in Fig. 9.

Spatial and spectral aberrations are in this case not negligible, and are the actual limit to the SOCS performance. Spatial aberrations are almost constant

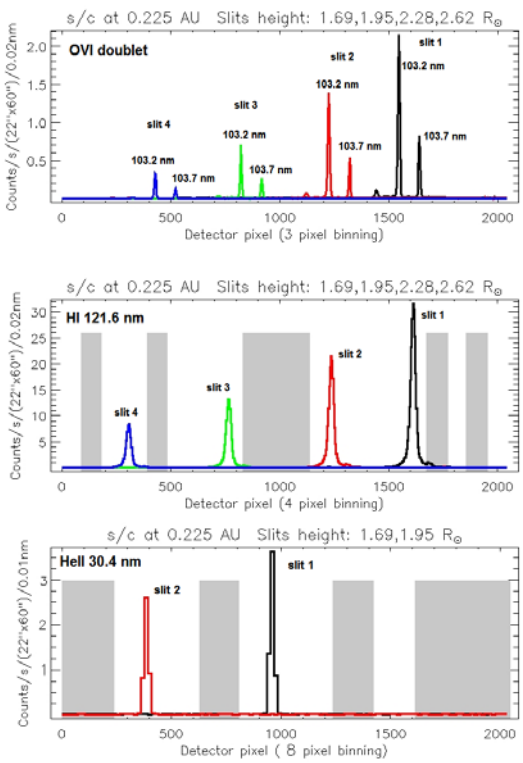

Fig. 8. Multiple spectra on the detectors provided by the multiple slit system. Top: channel 1, 1st order OVI 103.2-103.7 nm doublet; four slits visible. Mid: channel 2, 1st order HI Ly-α 121.6 nm; four slits visible. Bottom: channel 3, 5th order HeII 30.4 nm; two slits visible. The grey portions show the uncoated areas on the detector MCPs.

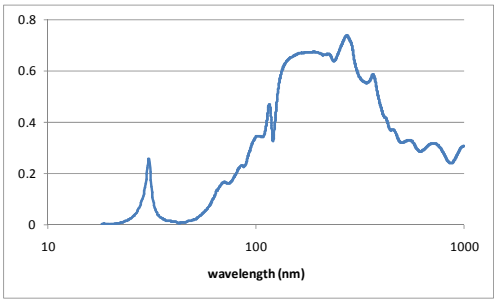

Fig. 9. Reflectivity curve of a Mo-Si multilayer mirror. Parameters: 16.5 nm period, gamma 0.85, 25 periods, SiO_2 cap-layer.

within the instantaneous FOV and depend on the slit: they are about 20 arcsec for slit #4, and increase up to 60 arcsec for slit #1. Spectral aberrations are equivalent to about 18, 20 and 5.3 pm for channels 1, 2 and 3, respectively.

The effective area of SOCS has been estimated taking into account the multilayer coating reflectivity, the grating diffraction efficiency, and the vignetting function. The grating peak diffraction efficiency has been assumed to be 50%, that is well within the present capabilities of the grating manufacturers. The multilayer reflectivity has been assumed to be 0.25 @ 30.4 nm and 0.30 @ 103.2 and 121.6 nm, accordingly with present measurements on Mo-Si coatings. The vignetting function depends on both the angular distance from the Sun and the off-axis observation angle, introducing a variation in the effective area of approximately a factor 3. The obtained values of the SOCS effective area range from 2-3 mm^2 for channel 3, to 2.5-7 mm^2 for channel 1, to 3-10 mm^2 for channel 2.

3. INTENSIFIED DETECTORS

EUS and SOCS share the same detectors, based on the Intensified Active Pixel Sensor (IAPS) architecture. COR UV detector is also an IAPS.

EUS and SOCS observe in two completely different intensity regimes: in fact, EUS looks at the disk while SOCS looks at the extended corona. Since there are orders of magnitude of different light intensities between these two regions, the common detectors need to have an extremely large dynamic range. The UV COR channel, instead, which observes only the corona, does not require such a large dynamic range.

An IAPS (see Fig. 10) consists of an MCP intensifier with phosphor screen output, optically coupled via fiber optic to an APS sensor [17,17]. A photocathode deposited on the entrance MCP face converts the incoming photons in primary photoelectrons, which are first multiplied by the MCP and then converted into optical photons by the phosphor screen. At the end of the process, the APS detects these optical photons. Thanks to this photon conversion process, an important characteristics of IAPS is their insensitivity to visible light (solar blind detector): this is a great advantage with respect, for instance, CCD detectors, with which metallic filters have to be adopted to block this unwanted light.

IAPS detectors have the capability to satisfy the described count rate requirements via operation in two different modes, integration and photon counting, suitable, respectively, for low and high level of flux. MCP intensifiers, indeed, can be operated in two different modes by changing their operating voltage: if the voltage across the channels of the MCP is below some threshold, the MCP works at low gain and the number of electrons at the output is proportional to the number of electrons at the input (analog or integration mode); if the voltage is higher than the threshold, saturation effects dominate and each photoelectron produces a charge that can be suitably detected as a single event (photon counting mode).

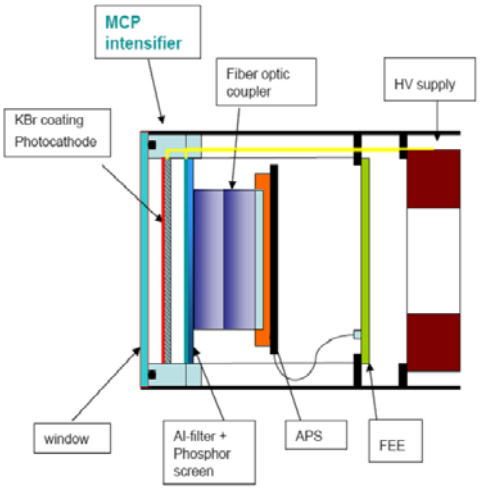

Fig. 10. Schematic of an IAPS detector.

At the same time, the APS readout system has to be suited for both operating modes. In analog mode, the APS is operated in "integration", accumulating enough signal to guarantee a good SNR. In photon counting mode, the APS is operated at a frame rate fast enough not to have overlapping of the spots generated by each photon; then each frame is searched to recognize these spots and return the event coordinates. This will be realized by the Front End Electronics (FEE) that will include the APS controller, which provides the digital signal sequences to operate the sensor, and a digital data processing block. The latter will implement different functions for the two operating modes: it will acquire the digital outputs looking for pixels over-threshold (corresponding to the photon events) to then accumulate the counts in an array, if working in photon counting mode; it will simply sum set of frames if working in analog mode.

In photon counting mode, the spot size can be made small enough to minimize, if not eliminating, centroiding computation, and the intensifier can be optimized for minimum event size (photon counting)/maximum limiting resolution (analog).

Due to the spectral ranges of COR, EUS and SOCS (where there is no transparent material to realize a window to work with a sealed detector), all the detectors will be in open configuration: the intensifier will be hosted in a vacuum housing with a door to be opened once in orbit and when in operation during the laboratory characterization and calibration phases.

4. CONCLUSIONS

METIS, the Multi Element Telescope for Imaging and Spectroscopy, an instrument proposed to the European Space Agency for the payload of the Solar Orbiter mission, has been briefly described. The instrument design has been conceived for performing EUV spectroscopy both on the solar disk and off-limb, and near-Sun coronagraphy and spectroscopy.

The proposed instrument suite consists of three different interconnected elements, COR, EUS and SOCS, sharing the same optical bench, electronics, and S/C heat shield aperture. COR is dedicated to the imaging observation of the solar corona in both visible, and Ly-α HI and HeII 30.4 nm lines. EUS and SOCS are strictly interconnected, and are dedicated to EUV spectroscopic observations, of both disk and corona.

This suite is a very challenging instrument, and many critical aspects have not been described here in detail. They range from the stray light rejection for observing the corona, to the huge dynamical range required to perform all these observations.

It is expected that ESA will select the instruments to be installed within the Solar Orbiter instrument bay within the end of the year.

ACKNOWLEDGEMENTS

Authors GD, DM, and JN wish to acknowledge the U.S. Naval Research Laboratory which supported them under the NRL 6.1 basic research funds.

REFERENCES

1. G. Naletto, et al., Optical design of a high spatial resolution extreme ultraviolet spectroheliograph for the transition region, *Appl. Opt.*, Vol. 44(24), 5046-5054, 2005.
2. F. Landini, et al., Stray-light analysis for the SCORE coronagraphs of HERSCHEL, *Appl. Opt.*, Vol. 45(26), 6657-6667, 2006.
3. Romoli, M., et al., The HERSCHEL/SCORE visible and UV coronagraph, ESA SP-641, on CD-ROM, 2007.
4. Fineschi, S., et al, KPol: liquid crystal polarimeter for K-corona observations from the SCORE coronagraph, *Proc. SPIE*, Vol. 5901, 389-399, 2005.
5. R.A. Frazin et al, White light intercalibrations of UVCS, LASCO-C2 and Spartan 201/WLC, *ESA SR-002*, 249, 2002.
6. J.L. Kohl et al., Ultraviolet spectroscopy of the extended corona, *Astron. Astrophys. Rev.*, Vol. 13, 31-157, 2006.
7. U. Schühle, et al., Thin silicon carbide coating of the primary mirror of VUV imaging instruments of Solar Orbiter, *ESA SP*-641, on CD-ROM, 2007.
8. R.J. Thomas, Toroidal varied line-space (TVLS) gratings, *Proc. SPIE*, Vol. 4853, 411-418, 2002.
9. L. Poletto and R.J. Thomas, Stigmatic spectrometers for extended sources: design with toroidal varied-line-space (TVLS) gratings, *Appl. Opt.*, Vol. 43, 2029-2038, 2004.

10. J.I. Larruquert and R.A.M. Keski-Kuha, Optical properties of hot-pressed B_4C in the extreme ultraviolet , *Appl. Opt.*, Vol. 39, 1537-1540, 2000.
11. G.M. Blumenstock and R.A.M. Keski-Kuha, Ion-beam deposited boron carbide coatings for extreme ultraviolet, *Appl. Opt.*, Vol. 33, 5962-5963, 1994.
12. O.H.W. Siegmund, et al., Ultraviolet quantum detection efficiency of potassium bromide as an opaque photocathode applied to microchannel plates, *Appl. Opt.*, Vol. 26, 3607-3614, 1987.
13. J.I. Larruquert, et al., Optical properties and quantum efficiency of thin-film alkali halides in the far ultraviolet, *Appl. Opt.*, 41, 2532-2540, 2002.
14. D.L. Windt, et al., Experimental comparison of extreme-ultraviolet multilayers for solar physics, *Appl. Opt.*, Vol. 43, 1835-1848, 2004.
15. M.-G. Pelizzo, et al., Design, deposition, and characterization of multilayer coatings for the Ultraviolet and Visible-Light Coronagraphic Imager, *Appl. Opt.*, Vol. 43, 2661-2669, 2004.
16. H. Takenaka, et al., Soft-X-ray reflectivity and heat resistance of SiC/Mg multilayer, *J. Electr. Spectr. Rel. Phen*., Vol. 1047, 144-147, 2005.
17. M. Uslenghi, et al., Characterization of a photon-counting intensified active pixel sensor (PC-IAPS): preliminary results, *Proc. SPIE*, Vol. 4498, 185-196, 2001.
18. G. Bonanno, et al., Photon counting system based on intensified CMOS-APS: PC-IAPS, *Proc. SPIE*, Vol. 4498, 173-184, 2001.